Orientation and alignment effects in electron-induced ionization of a single oriented water molecule

C. Champion[1,*] and R. D. Rivarola[2]

[1]*Laboratoire de Physique Moléculaire et des Collisions, ICPMB (FR CNRS 2843),Université Paul Verlaine-Metz, 1 boulevard Arago, F-57078 Metz Cedex 3, France*

[2]*Instituto de Física Rosario, CONICET and Universidad Nacional de Rosario, Avenida Pellegrini 250, 2000 Rosario, Argentina*

(Received 18 May 2010; published 11 October 2010)

We here report a theoretical study about the orientation effect on the total ionization cross sections for a single oriented water molecule. The theoretical description of the ionization process is performed within the first Born framework with a collisional system including an initial state composed of a projectile and a water target molecule described by a plane wave and an accurate one-center molecular wave function, respectively, and a final state constituted by a slow ejected electron represented by a Coulomb wave and a scattered (fast) electron projectile described by a plane wave. Secondary electron energetic distributions as well as total cross sections are then compared for particular target configurations pointing out strong alignment and orientation effects on the description of the ionization process.

DOI: 10.1103/PhysRevA.82.042704 PACS number(s): 34.50.Gb, 34.10.+x

I. INTRODUCTION

Target orientation effects on electron-induced ionization and fragmentation of molecules have been the subject of scarce experimental as well as theoretical investigations. In a general way, for high-enough projectile velocities, the reaction time τ ($\cong 10^{-16}$ s) remains considerably shorter than the rotational and vibrational periods of the molecules which permits us to assume that the impacted target molecule remains frozen during the collision [1,2]. Under these conditions, for the case of diatomic targets, the initial orientation of the molecular axis can be experimentally derived from the measured fragment velocity vectors and the ionization cross section studied as a function of the alignment of the molecular axis with respect to the electron beam. On this matter, this progress is essentially due to the use of the coincidence multihit cold-target recoil-ion-momentum spectroscopy (COLTRIMS) imaging technique, which made possible the study of the different dissociation channels with, in particular, the momentum detection of the target fragments following molecular dissociation [3].

The existing studies remain, up to now, essentially focused at the multidifferential scale for simple molecules like H_2 impacted by electrons [4] or positrons [5] and to the best of our knowledge only a few studies have reported total ionization cross sections for oriented molecules since the pioneering works of Kasai *et al.* [6] dedicated to indirect ionization induced by a 700 eV electron beam. Furthermore, let us cite the more recent work of Aitken *et al.* [7] where the authors investigated the ionization of the prolate symmetric top molecule CH_3Cl impacted by 200 eV electrons to determine the production of the molecular CH_3Cl^+ and the fragmentation product CH_3^+. The ionization cross section for the CH_3Cl^+ formation was then found higher at the positive end of the molecule whereas the observed cross section for the formation of the CH_3^+ fragmentation product was relatively independent of the target orientation. On the theoretical side, let us mention the recent work provided by Kretinin *et al.* [8] where total inelastic and integrated cross sections were reported within a Born-Bethe-type approximation and that performed by Gorfinkiel and Tennyson [9] where cross sections for the electron impact ionization of H_3^+ and H_2 molecules were determined by using the molecular *R*-matrix method with pseudostates. Finally, the orientation effect on single-electron-induced ionization was also studied by Stia *et al.* [10] who pointed out that the interference structures coming from the two-center geometry of the target molecule, namely, the H_2 molecule, were markedly dependent on the molecular orientation as already observed by other authors for heavy ion impact [11].

For single oriented water molecules there are no investigations except the very recent three-dimensional mapping of photoemission provided by Yamazaki *et al.* [12] in which the O_{1s} photoelectron angular distributions from a single oriented H_2O molecule were studied in detail. The experimental results also obtained within the quadruple coincidence framework clearly revealed the anisotropic feature of the photoionization dynamics. The lack of experimental information makes reliable theoretical predictions valuable. In this context, we have previously reported multidifferential cross sections for the $(e,2e)$ process on a single oriented water molecule within the framework of the first Born approximation and clearly identified a molecular orientation effect on the angular distributions of the secondary ejected electron for three particular geometric configurations, namely, a "parallel," an "antiparallel," and a "perpendicular" configuration which correspond to three target positions differing by the position of the hydrogen atoms with respect to the incident electron beam. Secondary electron angular distributions were then investigated in detail for each ionized molecular subshell via eightfold differential cross-section calculations and have evidently demonstrated their relative predominance with respect to the target orientation [13,14].

In the present work, we aim to point out that the molecular orientation is still crucial when less differential ionization cross sections are investigated, namely, in terms of secondary electron energy distributions (and more particularly the mean kinetic energy transfer) and total cross sections.

In the sequel, we deal with the theoretical model developed here for calculating the total ionization cross sections for

*Corresponding author: champion@univ-metz.fr

a single oriented water molecule impacted by electrons. The obtained results are then reported and analyzed and a conclusion about the influence of the molecular orientation on the ionization process is drawn.

In the following sections atomic units (a.u.) are used throughout unless indicated otherwise.

II. THEORY

The water molecule ionization process considered here can be schematized by

$$e^- + H_2O \rightarrow 2e^- + H_2O^+, \tag{1}$$

and regarded as a pure electronic transition since the closure relation over all possible rotational and vibrational states of the residual target can be applied. This assumption is completely justified by the previously reported relation between the collision time τ and the characteristic rotation and vibration times [2]. Furthermore, the scattered electron being always faster than the ejected one (for all the kinematical configurations here investigated), we will neglect the exchange effects in the theoretical approach developed in the following. These latter can be nevertheless included in further developments via, for example, the inclusion of the Gamow factor as previously done in [15].

Thus, similarly to our previous studies devoted to water molecule ionization by charged particles [16–18], the oriented water molecule is here described by means of single-center molecular wave functions [19,20] whose angular and radial parts are expressed by real solid harmonics [21] and Slater-type functions, respectively. The ten bound electrons of the water target molecule are then distributed among N (= 5) molecular orbitals, referred to in the following by their spectroscopic denomination $1b_1$, $3a_1$, $1b_2$, $2a_1$, and $1a_1$, whose corresponding ionization potentials are 0.4954, 0.5561, 0.6814, 1.3261, and 20.5249, respectively (for more details we refer the reader to our previous works [13–17]).

In this context and following the terminology used in [13], we have first calculated the eightfold differential cross sections (denoted in the following 8DCS), namely differential in the energy of the ejected electron E_e, differential in the direction of the ejected electron Ω_e, differential in the direction of the scattered particle Ω_s, and differential in the molecular orientation Ω_{Euler}, this latter being expressed by means of the Euler angle triplet (α,β,γ) via $d\Omega_{\text{Euler}} = \sin\beta\, d\alpha\, d\beta\, d\gamma$. Within the first Born approximation, the 8DCS are then expressed as

$$\frac{d^8\sigma}{dE_e d\Omega_e d\Omega_s d\Omega_{\text{Euler}}} = \sum_{j=1}^{5} \frac{d^8\sigma_j}{dE_e d\Omega_e d\Omega_s d\Omega_{\text{Euler}}} = \frac{1}{(2\pi)^5} \sum_{j=1}^{5} \frac{k_e k_s}{k_i} \left|[T_{if}]_j\right|^2, \tag{2}$$

where the momenta $\boldsymbol{k}_i$, $\boldsymbol{k}_s$, and $\mathbf{k}_e$, respectively, related to the incident, the scattered, and the ejected electron, depend on the corresponding energies through the relations $k_i^2 = 2E_i$, $k_e^2 = 2E_e$, and $k_s^2 = 2E_s$.

Under these conditions and keeping in mind that we describe here the incident and the scattered electrons by a plane wave and the ejected one by a Coulomb wave, Eq. (2) takes the convenient form

$$\frac{d^8\sigma}{dE_e \Omega_e d\Omega_s d\Omega_{\text{Euler}}} = \sum_{j=1}^{N=5} \frac{d^8\sigma_j}{dE_e \Omega_e d\Omega_s d\Omega_{\text{Euler}}} = \sum_{j=1}^{N=5} \frac{128\pi \cdot k_s}{k_e q^4 k_i} * \left| \begin{array}{l} \displaystyle\sum_{k=1}^{N_j} \sum_{l_e,l,m_e,m} i^{l-l_e} e^{i\sigma_{l_e}} \cdot X_{jk}^{l,l_e} \cdot Y_{l_e}^{m_e}(\hat{k}_e) \cdot Y_l^{m^*}(\hat{q}) \cdot \sum_{\mu=-l_{jk}}^{l_{jk}} \Delta_{l_{jk},m_{jk},\mu}(\alpha,\beta,\gamma) \cdot A_{l_e,m_e,l,m}^{l_{jk},\mu} \\ \displaystyle -\frac{1}{4\pi} \sum_{k=1}^{N_j} X'_{jk} \cdot \sum_{\mu=-l_{jk}}^{l_{jk}} \Delta_{l_{jk},m_{jk},\mu}(\alpha,\beta,\gamma) \cdot Y_{l_{jk}}^{\mu}(\hat{k}_e) \cdot i^{-l_{jk}} \cdot e^{i\sigma_{l_{jk}}} \end{array} \right|^2, \tag{3}$$

with

$$\Delta_{l_{jk},m_{jk},\mu}(\alpha,\beta,\gamma) = \frac{D_{\mu,-m_{jk}}^{l_{jk}}(\alpha,\beta,\gamma) - D_{\mu,m_{jk}}^{l_{jk}}(\alpha,\beta,\gamma)}{\sqrt{2}} \quad \text{if } j = 1 \ \ (i.e.\ \text{for the } 1b_1 \text{ orbital}),$$

$$\Delta_{l_{jk},m_{jk},\mu}(\alpha,\beta,\gamma) = i.\frac{D_{\mu,m_{jk}}^{l_{jk}}(\alpha,\beta,\gamma) + D_{\mu,-m_{jk}}^{l_{jk}}(\alpha,\beta,\gamma)}{\sqrt{2}} \quad \text{if } j = 3 \ \ (i.e.\ \text{for the } 1b_2 \text{ orbital}),$$

$$\Delta_{l_{jk},m_{jk},\mu}(\alpha,\beta,\gamma) = \frac{D_{\mu,m_{jk}}^{l_{jk}}(\alpha,\beta,\gamma) + D_{\mu,-m_{jk}}^{l_{jk}}(\alpha,\beta,\gamma)}{\sqrt{2}}\delta_{m_{jk},2} + D_{\mu,m_{jk}}^{l_{jk}}(\alpha,\beta,\gamma)\delta_{m_{jk},0} \quad \text{otherwise.}$$

Note that all information about the molecular orientation is included in the rotation matrix $D_{\mu,m_{jk}}^{l_{jk}}(\alpha,\beta,\gamma)$ given by

$$D_{\mu,m_{jk}}^{l_{jk}}(\alpha,\beta,\gamma) = e^{-im_{jk}\alpha} d_{\mu,m_{jk}}^{l_{jk}}(\beta) e^{-i\mu\gamma}, \tag{4}$$

where $d_{\mu,m_{jk}}^{l_{jk}}(\beta)$ is given by the Wigner formula

$$d_{\mu,m_{jk}}^{l_{jk}} = \sum_{t=0}^{\tau} (-1)^t \frac{\sqrt{(l_{jk}+\mu)!(l_{jk}-\mu)!(l_{jk}+m_{jk})!(l_{jk}-m_{jk})!}}{(l_{jk}+\mu-t)!(l_{jk}-m_{jk}-t)!t!(t-\mu+m_{jk})!} \xi^{2l_{jk}+\mu-m_{jk}-2t} * \eta^{2t-\mu+m_{jk}}, \quad \text{with} \quad \begin{cases} \xi = \cos(\beta/2), \\ \eta = \sin(\beta/2). \end{cases} \tag{5}$$

The symbols $X_{jk}^{l,l_e}, X'_{jk}, A_{l_e,m_e,l,m}^{l_{jk},\mu}$ reported in Eq. (3) are given by

$$A_{l_e,m_e,l,m}^{l_{jk},\mu} = (-1)^{m_e}\sqrt{\frac{\hat{l}_e\hat{l}\hat{l}_{jk}}{4\pi}}\begin{pmatrix} l_e & l & l_{jk} \\ 0 & 0 & 0 \end{pmatrix}\begin{pmatrix} l_e & l & l_{jk} \\ -m_e & m & \mu \end{pmatrix} \quad \text{with} \quad \hat{l} = 2l+1, \tag{6}$$

$$X_{jk}^{l,l_e} = \int_0^\infty dr\, r\, F_{l_e}(k_e,r)\, j_l(qr)\, f_{jk}(r), \tag{7}$$

and

$$X'_{jk} = \int_0^\infty dr\, r\, F_{l_{jk}}(k_e,r)\, f_{jk}(r), \tag{8}$$

where $\boldsymbol{q} = \boldsymbol{k}_i - \mathbf{k}_s$ denotes the transfer momentum.

In Eqs. (7) and (8), $F_l(k_e,r)$ denotes the well-known radial regular function whereas $j_l(qr)$ and $f_{jk}(r)$ represent the Bessel function and the radial part of the kth component of the jth molecular orbital, respectively. Furthermore, note that in Eq. (3) σ_l represents the Coulomb phase shift.

In a subsequent step, 6DCS are obtained via an analytical integration of the 8DCS over the ejection direction $\Omega_e \equiv \widehat{k_e}$. These latter may be simply expressed as

$$\begin{aligned}\frac{d^6\sigma}{dE_e d\Omega_s d\Omega_{\text{Euler}}} &= \sum_{j=1}^{N=5}\frac{d^6\sigma_j}{dE_e d\Omega_s d\Omega_{\text{Euler}}} = \sum_{j=1}^{N=5}\int\frac{d^8\sigma_j}{dE_e d\Omega_e d\Omega_s d\Omega_{\text{Euler}}}d\Omega_e \\ &= \sum_{j=1}^{N=5}\frac{128\pi k_s}{k_e q^4 k_i}\left\{\sum_{l_e,m_e}\left|\sum_{k=1}^{N_j}\sum_{l,m}X_{jk}^{l,l_e}Y_l^{m*}(\hat{q})\begin{pmatrix} l_e & l & l_{jk} \\ 0 & 0 & 0 \end{pmatrix}\begin{pmatrix} l_e & l & l_{jk} \\ -m_e & m & m_e-m \end{pmatrix} i^l\sqrt{\frac{\hat{l}_e\hat{l}\hat{l}_{jk}}{4\pi}}\Delta_{l_{jk},m_{jk},m_e-m}\right|^2\right. \\ &\quad + \frac{1}{(4\pi)^2}\sum_{k=1}^{N_j}(X'_{jk})^2 \\ &\quad \left. + 2\text{Re}\left[\frac{(-1)}{4\pi}\sum_{k,k'=1}^{N_j}\sum_{l,m}X_{jk}^{l,l_{jk'}}X'_{jk'}Y_l^{m*}(\hat{q})\, i^l\sqrt{\frac{\hat{l}\hat{l}_{jk}\hat{l}_{jk'}}{4\pi}}\sum_{\mu=-l_{jk'}}^{+l_{jk'}}(-1)^\mu\begin{pmatrix} l_{jk'} & l & l_{jk} \\ 0 & 0 & 0 \end{pmatrix}\begin{pmatrix} l_{jk'} & l & l_{jk} \\ -\mu & m & \mu-m \end{pmatrix}\right]\right\},\end{aligned} \tag{9}$$

where Re[z] denotes the real part of the complex z.

Finally, total ionization cross sections for a single oriented water molecule, namely, the differential cross sections referred to as $\frac{d^3\sigma}{d\Omega_{\text{Euler}}}$, are then obtained by numerical integrations of the 6DCS over the scattered direction $\Omega_s \equiv \widehat{k_s}$ and the kinetic energy transfer E_e.

III. RESULTS AND DISCUSSION

The present work aims to highlight the influence of the molecular target orientation on the ionization process. To do that, we investigate here the particular orientations of the water molecule defined by means of the Euler angles (α,β,γ) from an initial orientation $(\alpha,\beta,\gamma) = (0,0,0)$, which corresponds to a molecule sited in the yz plane with its bisecting line along the z axis (see Fig. 1), and obtained by a β rotation around the y axis (with β ranging from 0 to $\pi/2$) by keeping $\alpha = \gamma = 0$. This transformation will be denoted $R_y(0,\beta,0)$ in the following. Finally, note that in all the cases investigated here the incident momentum $\boldsymbol{k}_i$ is collinear to the z axis.

Studying the orientation effects on the ionization process for a single oriented molecule requires discriminating each

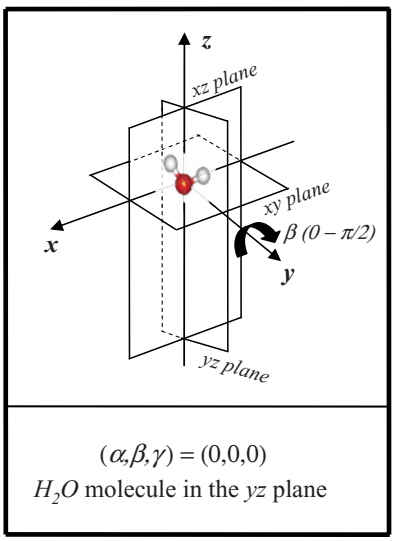

FIG. 1. (Color online) Schematic representation of the initial water molecule orientation $(\alpha,\beta,\gamma) = (0,0,0)$ as well as the particular rotation $R_y(0,\beta,0)$ investigated in the present work.

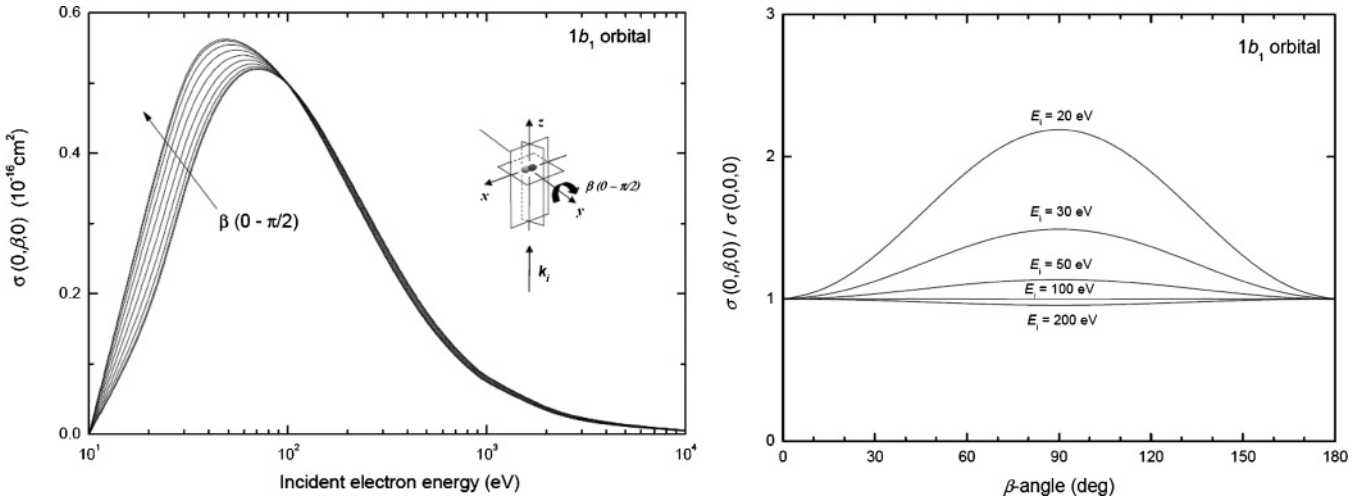

FIG. 2. Left panel: Total ionization cross sections of the $1b_1$ molecular orbital for particular orientations defined by the β angle (ranging from 0 to $\pi/2$). Right panel: Variation of the total ionization cross sections of the $1b_1$ molecular orbital with the β angle for several incident energies. Curves are normalized at $\beta = 0$.

molecular subshell contribution, this latter being dependent on the relative alignment of the impacted orbital with respect to the incident beam. Under these conditions, we successively report in the following a detailed exam of the ionization of each of the four outermost subshells of the water molecule for a target orientation defined via the $R_y(0,\beta,0)$ rotation with β ranging from 0 to $\pi/2$.

Let us first consider the outer molecular subshell, namely, the $1b_1$ orbital. This latter is mainly governed by a $2p_{+1}$ orbital ($\approx$99.57%) and then corresponds, in the present molecular description based on *real solid harmonics*, to an orbital collinear to the x molecular axis (see [36] for more details). This orbital type will be denoted P_X in the following. Thus, applying the $R_y(0,\beta,0)$ rotation on the $1b_1$ orbital means going from an initial configuration where the orbital is sited on the xy plane to a final configuration where the orbital is sited on the yz plane, as shown below in Eq. (10) where the $R_y(0,\beta,0)$ transformations were summarized

$$R_y(0,\pi/2,0): \begin{cases} P_X \rightarrow P_Z, \\ P_Y \rightarrow P_Y, \\ P_Z \rightarrow P_X. \end{cases} \tag{10}$$

Figure 2 (left panel) reports the calculated total ionization cross sections for the $1b_1$ orbital. The evident influence of the orbital alignment on the ionization process may be observed, in particular, in magnitude. Indeed, it clearly appears that at low and intermediate collision energies ($E_i < 100$ eV) the highest cross sections are obtained when the impacted orbital is collinear to the beam axis (the z axis), namely, for $\beta = \pi/2$ whereas at high collision energies ($E_i > 100$ eV), the highest cross sections are observed for $\beta = 0$ for a target orbital perpendicular to the beam axis. This previously reported behavior can be simply explained by geometrical considerations. Thus, at low and intermediate energies, the incident electron is sensitive to the orientation of the impacted orbital and the ionization process is privileged when the orbital is aligned with the incident electron momentum revealing then a direct reflection of the anisotropic distributions of the electron density of the impacted molecular orbital. On the contrary, as the electron energy increases, the ionization process is dominant when the target orbital is perpendicular to the incident beam (i.e., when the geometrical cross section is the highest), which meets the observations already made by many authors studying ion-induced ionization of diatomic molecules who reported a slight increase at perpendicular orientation of the target molecule [21]. This particular feature is clearly highlighted in Fig. 2 (right panel) where the variation of the ratio $\sigma(0,\beta,0)/\sigma(0,0,0)$ versus the β angle for different incident energies is reported.

Furthermore, in Fig. 2 (left panel), we also observe that the position of the maxima, denoted $E_i^{\max}$, is shifted toward the low incident energies all the more that the impacted orbital tends to be aligned with the axis beam. Thus, we find that $E_i^{\max}$ ranges from 48 eV for the parallel orientation ($\beta = \pi/2$) to 72 eV for the perpendicular orientation ($\beta = 0$). This behavior can also be interpreted from Fig. 2 (right panel) where it is shown that the main contribution at perpendicular orientation comes from the lower impact energies producing thus the corresponding shift in the position of the maxima.

Considering the $3a_1$ orbital whose major component is $2p_0$ ($\approx$93.36%, the remaining being essentially governed by a $1s$-$2s$ component $\approx$5.14%) denoted P_Z in the following, we obviously observe the opposite trends. Indeed, following the transformations of the $R_y(0,\beta,0)$ rotation reported in Eq. (10) according to which a P_Z orbital becomes a P_X one, it is evident that the present orbital is rotated from the yz plane to the xy plane. In these conditions, the $3a_1$ orbital, initially aligned with the incident electron beam, now becomes perpendicular to the incident electron momentum ($\beta = \pi/2$), which leads to total cross sections whose maxima are located at ($\beta = 0$) for an orbital orientation parallel to the incident beam at low and intermediate collision velocities whereas at high impact velocities the cross sections are dominated for perpendicular alignment to the incident beam ($\beta = \pi/2$). Note that the low $1s$-$2s$ contribution is obviously not concerned by the β-angle

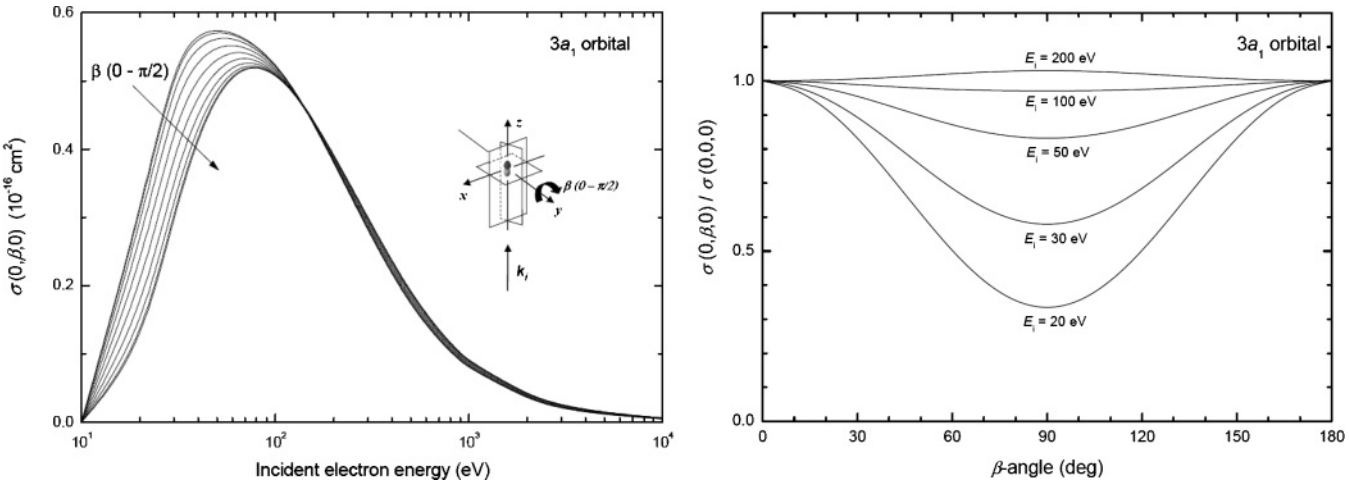

FIG. 3. Left panel: Total ionization cross sections of the $3a_1$ molecular orbital for particular orientations defined by the β angle (ranging from 0 to $\pi/2$). Right panel: Variation of the total ionization cross sections of the $3a_1$ molecular orbital with the β angle for several incident energies. Curves are normalized at $\beta = 0$.

rotation and therefore does not participate in this alignment effect (see Fig. 3).

A similar study has also been performed for the $1b_2$ molecular state mainly governed by a $2p_{-1}$ orbital (≈93.75%) and therefore denoted P_Y in the following. In this case, it is clear that the rotation $R_y(0,\beta,0)$ will not change the orientation of the molecular orbital, which then remains aligned with the y axis. However, the calculated total cross sections exhibit a slight dependence versus the target orientation that may be explained by the fact that the $1b_2$ orbital is not a pure $2p_{-1}$ molecular state, but presents a nonnegligible $3d_{-1}$ component (≈5.63%), which corresponds in the present real solid-harmonics-based description to four lobes sited in the yz plane. In these conditions, this "extra" component appears as in the collision plane for $\beta = 0$, whereas it is perpendicular to the incident electron beam for $\beta = \pi/2$, which results at low and intermediate collision velocities in a minimum for the ionization probability located at $\beta = \pi/2$ as observed in Fig. 4. Once more, we observe that the perpendicular orientation dominates when the impact energy increases.

Finally, the $2a_1$ molecular state, mainly governed by a $1s$-$2s$ component (≈95.30%) with nevertheless a nonnegligible $2p_0$ (i.e., a P_Z) contribution (≈3.77%), shows a pronounced minimum for $\beta = \pi/2$ at low and intermediate impact energies, whose explanation is similar to that given previously for the $1b_2$ orbital, namely, a minimal total ionization cross section observed for a perpendicular orientation of the low $2p_0$ component (i.e., for $\beta = \pi/2$). This minimum appears to be more pronounced as the incident electron energy is low. This is coherent with the above-reported remark according to which the electron is more sensitive to the particular orientation of the impacted orbital as its incident energy is low. For high impact energies (i.e., for $E_i > 300$ eV) a slight increase

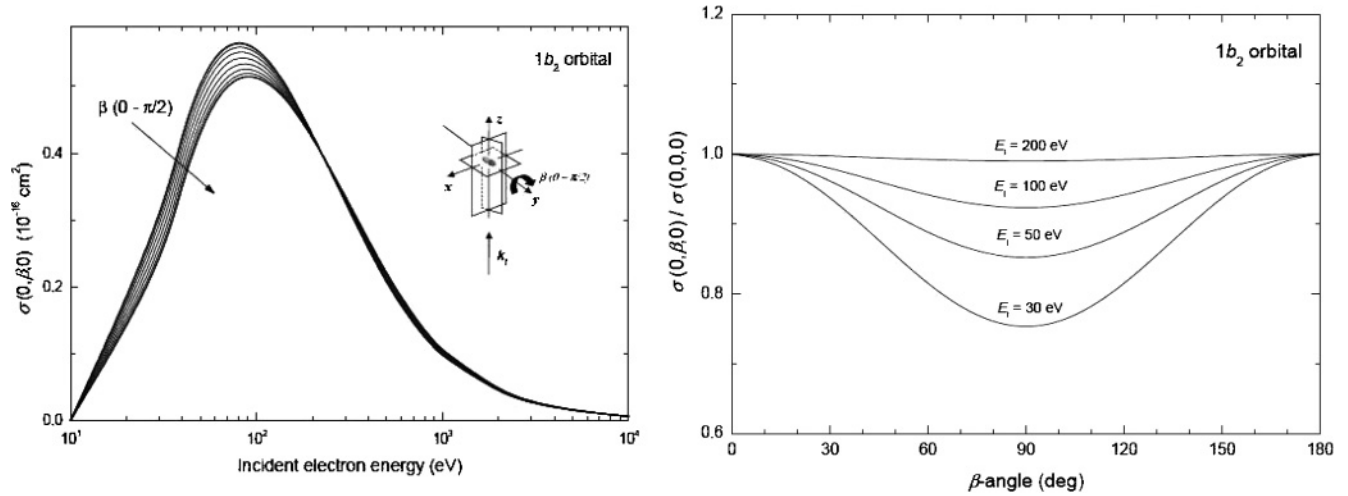

FIG. 4. Left panel: Total ionization cross sections of the $1b_2$ molecular orbital for particular orientations defined by the β angle (ranging from 0 to $\pi/2$). Right panel: Variation of the total ionization cross section of the $1b_2$ molecular orbital with the β angle for several incident energies. Curves are normalized at $\beta = 0$.

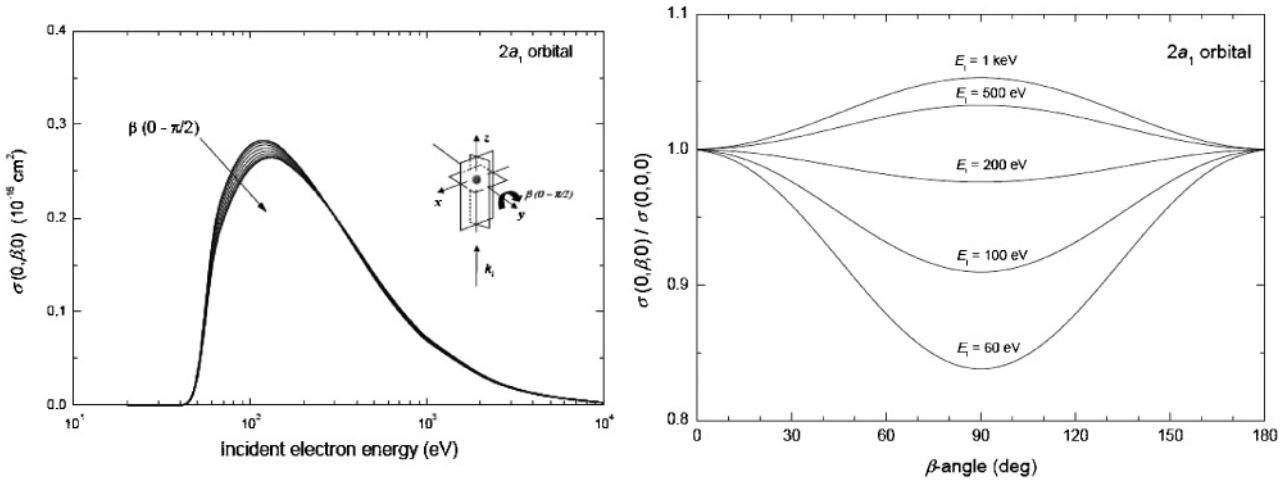

FIG. 5. Left panel: Total ionization cross sections of the $2a_1$ molecular orbital for particular orientations defined by the β angle (ranging from 0 to $\pi/2$). Right panel: Variation of the total ionization cross section of the $2a_1$ molecular orbital with the β angle for several incident energies. Curves are normalized at $\beta = 0$.

is shown at $\beta = \pi/2$ in Fig. 5 (right panel), which is coherent with the previous observations as well as those reported by many authors for ion-induced ionization of diatomic molecules [21].

Correlatively, it seemed pertinent to us to study the variation of the mean kinetic energy transferred $\langle E_e \rangle$ during the ionization process as a function of the relative orientation of the ionized orbital. Figure 6 reports the calculated mean

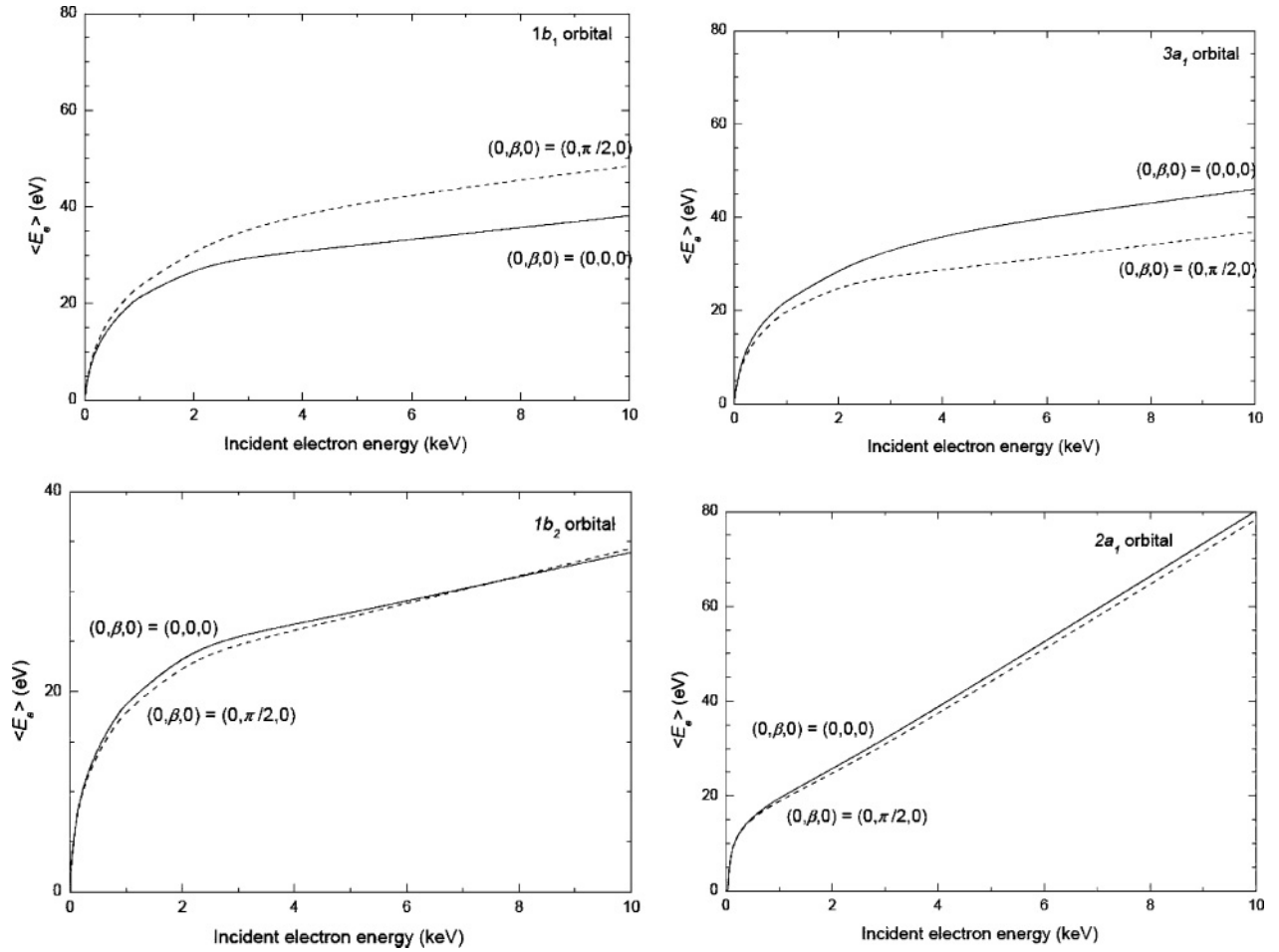

FIG. 6. Variation of the mean kinetic energy $\langle E_e \rangle$ released during the ionization process versus the incident electron energies for the four outermost water molecular orbitals and for the two extreme β-angle values here investigated, namely, $\beta = 0$ and $\beta = \pi/2$.

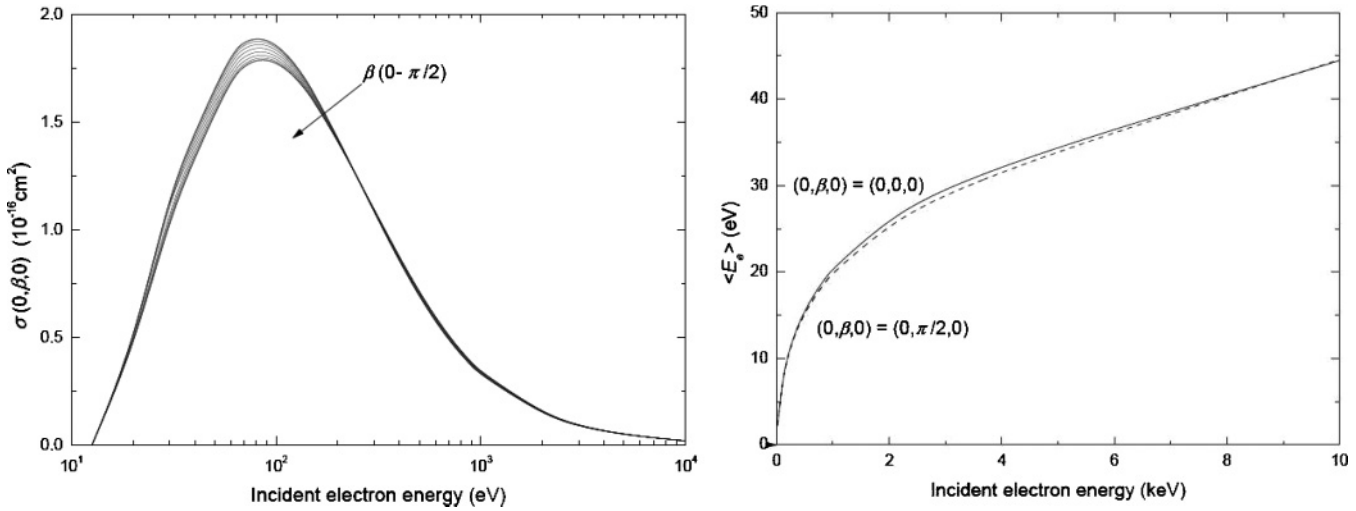

FIG. 7. Left panel: Total ionization cross sections of the water molecule for particular orientations defined by the β angle (ranging from 0 to $\pi/2$). Right panel: Variation of the mean kinetic energy released during the ionization of the water molecule with the incident energies for the two extreme values of the β angle here investigated $\beta = 0$ and $\beta = \pi/2$.

kinetic energy transferred during the collision as a function of the β angle deduced from the oriented singly differential cross sections, these latter being obtained after integration over all possible ejected electron momenta. A strong alignment effect on the energy deposition may be observed, undoubtedly originating from the anisotropy of the electron density distribution. Thus, on the basis of a simple physical argument, we observe that the kinetic energy transfer is greater when the orbital is aligned with the incident beam ($\beta = \pi/2$ and $\beta = 0$ for the $1b_1$ and the $3a_1$ orbital, respectively), giving then an estimation on the close encounter character of the collision since, in this case, the projectile has a higher probability to "encounter" target electrons and then to induce a higher kinetic-energy transfer. In fact, when the orbital is oriented along the beam, the probability of a large energy deposition is greater than for an orientation perpendicular to the beam because the projected electron density sampled by the projectile is larger. Moreover, it is clear that *for parallel alignment* the emission of faster electrons in the incident beam direction is facilitated considering that the secondary electrons will be preferentially ejected in the z direction. On the contrary, *for perpendicular alignment*, the mean kinetic energy transferred is smaller than for parallel orientation, indicating that the large encounter contributions may play an important role. This is in agreement with the geometrical interpretation of large cross sections at high impact velocities.

For the other orbitals, the mean kinetic energy transfers are slightly influenced by the orbital orientation and then exhibit a quasi-independence versus the β angle, namely, $0.99 < \frac{\langle E_e\rangle(0,0,0)}{\langle E_e\rangle(0,\pi/2,0)} < 1.04$ for the $1b_2$ orbital and $0.98 < \frac{\langle E_e\rangle(0,0,0)}{\langle E_e\rangle(0,\pi/2,0)} < 1.04$ for the $2a_1$ orbital (see Fig. 6). Nonetheless, let us note that here again, the maximum observed for these two cases correspond to the alignment of the minor molecular components, namely, the $3d_{-1}$ ($\approx$5.63%) and the $2p_0$ ($\approx$3.77%) ones with the electron beam, the major contributions (respectively, $2p_{-1}$ and $1s$-$2s$) remaining always perpendicular to the incident electron direction.

Let us mention that the inner shell $1a_1$ is not studied here since it exhibits a pure $1s$ component ($\approx$100%) and then leads to an isotropic total ionization cross section.

In Fig. 7, we report the summation of all the molecular subshell contributions to observe the overall behavior of the water molecule with respect to its orientation versus the incident electron beam. As expected, the contributions of the $1b_1$ and $3a_1$ molecular states annul each other leading to a final feature for the ionization of an oriented water molecule taken from the $1b_2$ and, in a lesser extent, from the $2a_1$ contributions. Thus, we obtain a maximal cross section for $\beta = 0$ (i.e., for a molecule sited in the yz plane) namely, the collision plane. Furthermore, the mean kinetic-energy transfers exhibit a quasi-independence versus the molecule orientation.

Finally, note that the total ionization cross sections obtained by averaging over all possible molecular orientations were shown to be in good agreement with the experimental data from 10 to 10 keV [17].

IV. CONCLUSION

The scope of the current work was to theoretically investigate how target orientation might affect the ionization process for isolated water molecules. In the first Born approximation and by using an accurate one-center molecular target wave function, we have here reported strong alignment effects, in particular when the water molecule ionization process was studied *orbital by orbital*. Indeed, for each molecular subshell the observations reported here in terms of preferential orientations for ionization induction as well as kinetic-energy transfers (δ electrons) were qualitatively explained.

Thus, we have shown that at low and intermediate collision energies ($E_i < 100$ eV) the ionization process was privileged for impacted orbitals aligned with the incident electron momentum revealing then a direct reflection of the anisotropic

distributions of the electron density of the molecular orbitals. It has also been reported that this effect was inverted for increasing projectile energies. This behavior has been also observed for low-degree ionization of diatomic molecular targets by ion impact. However, when "macroscopic" observations were made, namely, without discriminating the different molecular subshell contributions, we clearly exhibited that the ionization process was quasi-isotropic without any privileged water molecule direction.

Finally, note that at this stage no direct comparison with the experiment is possible and we hope that these current predictions will be in the near future confirmed by experimental observations.

ACKNOWLEDGMENTS

This work has been developed as a part of the activities planned in the Programme de Coopération ECOS-Sud A09E04. RDR acknowledges the Agencia Nacional de Promoción Científica y Tecnológica of República Argentina for partial financial support through the Project PICT No. 1912.

[1] P. Weck, B. Joulakian, J. Hanssen, O. A. Fojón, and R. D. Rivarola, Phys. Rev. A **62**, 014701 (2000).
[2] P. Weck, O. A. Fojón, J. Hanssen, B. Joulakian, and R. D. Rivarola, Phys. Rev. A **63**, 042709 (2001).
[3] J. Ullrich, R. Moshammer, A. Dorn, R. Dörner, L. Ph. H. Schmidt, and H. Schmidt-Böcking, Rep. Prog. Phys. **66**, 1463 (2003).
[4] J. Colgan, M. S. Pindzola, F. Robicheaux, C. Kaiser, A. J. Murray, and D. H. Madison, Phys. Rev. Lett. **101**, 233201 (2008).
[5] J. Fiol and R. O. Barrachina, J. Phys. B: At. Mol. Opt. Phys. **42**, 231004 (2009).
[6] T. Kasai, T. Matsunami, T. Fukawa, H. Ohoyama, and K. Kuwata, Phys. Rev. Lett. **70**, 3864 (1993).
[7] C. G. Aitken, D. A. Blunt, and P. W. Harland, J. Chem. Phys. **101**, 11074 (1994).
[8] I. Yu Kretinin, A. V. Krisilov, and B. A. Zon, J. Phys. B: At. Mol. Opt. Phys. **41**, 215206 (2008).
[9] J. D. Gorfinkiel and J. Tennyson, J. Phys. B: At. Mol. Opt. Phys. **38**, 1607 (2005).
[10] C. R. Stia, O. A. Fojón, P. F. Weck, J. Hanssen, and R. D. Rivarola, J. Phys. B: At. Mol. Opt. Phys. **36**, L257 (2003).
[11] G. Laurent, P. D. Fainstein, M. E. Galassi, R. D. Rivarola, L. Adoui, and A. Cassimi, J. Phys. B: At. Mol. Opt. Phys. **35**, L495 (2002).
[12] M. Yamazaki, J. Adachi, T. Teramoto, A. Yagishita, M. Stener, and P. Decleva, J. Phys. B: At. Mol. Opt. Phys. **42**, 051001 (2009).
[13] C. Champion, J. Hanssen, and P.-A. Hervieux, Phys. Rev. A **63**, 052720 (2001).
[14] C. Champion, J. Hanssen, and P.-A. Hervieux, Phys. Rev. A **72**, 059906(E) (2005).
[15] C. Champion, C. Dal Cappello, S. Houamer, and A. Mansouri, Phys. Rev. A **73**, 012717 (2006).
[16] D. S. Milne-Brownlie, S. J. Cavanagh, B. Lohmann, C. Champion, P.-A. Hervieux, and J. Hanssen, Phys. Rev. A **69**, 032701 (2004).
[17] C. Champion, J. Hanssen, and P.-A. Hervieux, J. Chem. Phys. **121**, 9423 (2004).
[18] C. Champion, O. Boudrioua, C. Dal Cappello, Y. Sato, and D. Ohsawa, Phys. Rev. A **75**, 032724 (2007).
[19] R. Moccia, J. Chem. Phys. **40**, 2186 (1964).
[20] R. Moccia, J. Chem. Phys. **40**, 2164 (1964).
[21] U. Werner, N. M. Kabachnik, V. N. Kondratyev, and H. O. Lutz, Phys. Rev. Lett. **79**, 1662 (1997).